International Journal of Greenhouse Gas Control 19 (2013) 299–309

Contents lists available at ScienceDirect

International Journal of Greenhouse Gas Control

journal homepage: www.elsevier.com/locate/ijggc

High pressure separation of greenhouse gases from air with 1-ethyl-3-methylimidazolium methyl-phosphonate

Luís M.C. Pereira[a], Mariana B. Oliveira[a], Ana M.A. Dias[b], Felix Llovell[c], Lourdes F. Vega[c,d], Pedro J. Carvalho[a], João A.P. Coutinho[a,*]

[a] CICECO, Departamento de Química, Universidade de Aveiro, 3810-193 Aveiro, Portugal
[b] CIEPQPF, Departamento de Engenharia Química, FCTUC, Universidade de Coimbra, Rua Sílvio Lima, Pólo II – Pinhal de Marrocos, 3030-790 Coimbra, Portugal
[c] MATGAS Research Center (Carburos Metálicos/Air Products, CSIC, UAB), Campus UAB, 08193 Bellaterra, Barcelona, Spain
[d] Carburos Metálicos/Air ProductsGroup, C/ Aragón, 300, 08009 Barcelona, Spain

ARTICLE INFO

Article history:
Received 21 December 2012
Received in revised form 4 September 2013
Accepted 9 September 2013

Keywords:
Ionic liquids
Gas solubilities
soft-SAFT modeling
Henry's constant
Selectivities

ABSTRACT

Increasing pollutants emissions, along with the limitations present on the existing control methods and stricter legislation to come, demand the development of new methods to reduce them. Ionic liquids (ILs) have been attracting an outstanding attention during the last decade and rose as a promising class of viable solvents to capture pollutants and for gas separation processes. As part of a continuing effort to develop an ionic liquid based process for high pressure capture of greenhouse gases, the phase equilibria of carbon dioxide (CO_2), nitrous oxide (N_2O), methane (CH_4) and nitrogen (N_2) in 1-ethyl-3-methylimidazolium methyl-phosphonate ($[C_2mim][CH_3OHPO_2]$) were studied in this work.

Experimental measurements for the CO_2, N_2O, CH_4 and N_2 solubilities in $[C_2mim][CH_3OHPO_2]$ were carried out for gases mole fractions ranging from (0.018 to 0.504), in the temperature range (293.23 to 363.34) K and for pressures from (1.16 to 87.61) MPa.

The particular behavior of the selected highly polar ionic liquid is here shown for the first time through the reported experimental data. The low N_2, CH_4 and CO_2 solubilities, with the later system presenting positive deviations to ideality, show the ionic liquid unfavorable interactions with the studied gases and the necessity to find a proper compromise between the solvent polarity and its molar volume in order to achieve high CO_2/N_2 or CO_2/CH_4 separation selectivities.

The good soft-SAFT EoS performance in describing the thermophysical properties of ionic liquids and the phase equilibria of their mixtures with gases was extended in this work for the description of the experimental data reported. New and reliable molecular schemes for N_2O and $[C_2mim][CH_3OHPO_2]$, not yet studied within the soft-SAFT framework, were proposed. Using no more than one binary interaction parameter, the soft-SAFT EoS is able to take into account the particular pressure and temperature behavior of the different gases solubilities in the selected ionic liquid. This empowers the equation to be reliably used for other similar systems, as tool to optimize the given process, searching for the best conditions for capture.

1. Introduction

Several sources, anthropogenic or of natural origin, contribute to the emission of several greenhouse gases into the atmosphere, with burning of fossil fuels and industrial processes having the highest negative impact. Among several post-combustion capture and natural gases treatment processes currently available to reduce these emissions, such as membrane-based separations and physical and chemical sorbents adsorption, the amines and ammonia absorption processes maintain a prominent position, with most of the industrial plants using chemical absorption processes with monoethanolamine (MEA)-based solvents. Although modified to incorporate inhibitors, that reduce solvent degradation and equipment corrosion, the MEA-based processes still present several disadvantages, such as large equipment sizes, due to low amines/water weight relation, high solvent regeneration costs and loss of solvent by evaporation, to mention just a few (Olajire, 2010). Furthermore, limitations on the existing control methods and on the industrial processes require the development of new methods and processes, to reduce the pollutants level.

Among all greenhouse gases, carbon dioxide (CO_2) nitrous oxide (N_2O) and methane (CH_4) are the most abundant and, hence, with

* Corresponding author. Tel.: +351 234 401 507; fax: +351 234 370 084.
E-mail address: jcoutinho@ua.pt (J.A.P. Coutinho).

1750-5836/$ – see front matter © 2013 Elsevier Ltd. All rights reserved.
http://dx.doi.org/10.1016/j.ijggc.2013.09.007

the higher impact on Earth's temperature. Methane and nitrous oxide are estimated to have an overall contribution to global warming of 23 and 296 times higher than carbon dioxide, respectively, over a 100-year time frame. In addition, nitrous oxide, the major input of nitrogen oxides compounds, is becoming an important regulator of stratospheric ozone and, therefore, the main responsible for the ozone depleting (Ravishankara et al., 2009). Presently, carbon dioxide accounts for 56.6% of total global anthropogenic greenhouse gas emissions, followed by methane with 14.3% and nitrous oxide with 7.9% (IPCC, 2007).

Ionic liquids (ILs), due to their outstanding characteristics, such as negligible flammability and vapor pressure, thermal stability and highly solvating capacity either for polar and non-polar compounds (Rogers and Seddon, 2003; Marsh et al., 2004; Chiappe and Pieraccini, 2005), and the aptness for fine-tuning of their properties by the appropriate combination of cation and anion stand as a viable alternative to replace commonly used solvents in natural gas and post-combustion treatments. In fact, ILs based liquid membranes, characterized by high fluxes and high selectivities, are being reported as a promising method for high pressure gas separation (Morgan et al., 2005; Poloncarzova et al., 2011; Scovazzo et al., 2009). Understanding the solubility of gases in ILs, in a wide range of molar fractions, temperature and pressures, is essential for the adequate development and optimization of these processes before they are put final use. Gas separation using IL-based membranes seems to be controlled by the gas solubility in the ionic liquid rather than by its diffusivity and therefore, the solubility of gases in ILs has received a great deal of attention in the past decade (Bara et al., 2009; Carvalho and Coutinho, 2010a; Ferguson and Scovazzo, 2007; Revelli et al., 2010a,b; Shiflett et al., 2010, 2012a,b; Yokozeki et al., 2008). However, the characterization of the ILs properties is still scarce and limited to a small number of ILs and ILs families, making its study of key importance for a correct design and optimization of industrial processes. In this work, the solubility of CO_2, N_2O, CH_4 and nitrogen (N_2) (used as a representative model of air) in 1-ethyl-3-methylimidazolium methyl-phosphonate ($[C_2mim][CH_3OHPO_2]$) is investigated for temperatures up to 363 K and pressures up to 100 MPa. In previous works (Carvalho and Coutinho, 2010a,b, 2011), the mechanism behind the sorption of several gases in ILs has been discussed and the hypothesis that the IL-gas selectivity is related to the IL polarity has been proposed. With the new data provided in this work for the solubilities of CO_2, N_2O, CH_4 and N_2 in a highly polar ionic liquid, this idea is further discussed.

The large number of cations and anions combinations limits the feasibility of the complete experimental ILs characterization. Thus, the development of reliable thermodynamic models capable of estimating the solubility of gases in ILs stands as a vital key on the pursuit of alternative solvents and processes. SAFT-type (Statistical Association Fluid Theory) equations of state (EoS) have successful and accurately provided reliable predictions for phase equilibria and thermophysical properties based on molecular model parameters established on statistical mechanics concepts with physical meaning and independent of the thermodynamic conditions. Moreover, SAFT-type EoS, namely the tPC-PSAFT (Arce and Aznar, 2007; Chen et al., 2012; Karakatsani et al., 2007; Kroon et al., 2006), the soft-SAFT (Andreu and Vega, 2007, 2008; Llovell et al., 2011, 2012a,b; Oliveira et al., 2012a,b; Vega et al., 2010) and the HeteroSAFT (Ji and Adidharma, 2009, 2010) versions, have already been applied with success to the gas solubility modeling on ILs, as well as other complex systems.

In particular, the soft-SAFT EoS has shown outstanding results modeling the thermophysical properties of ILs and their phase equilibria for a large number of gases and complex associating compounds in a large range of thermodynamic conditions (Andreu and Vega, 2007, 2008; Llovell et al., 2012a,b; Oliveira et al., 2012a,b; Vega et al., 2010). Considering phase equilibria description, Andreu and Vega applied the soft-SAFT EoS to successfully describe the solubility of CO_2 in 1-alkyl-3-methylimidazolium tetrafluoroborate $[C_nmim][BF_4]$ and in 1-alkyl-3-methylimidazolium hexafluorophosphate $[C_nmim][PF_6]$ ILs (Andreu and Vega, 2007), and the solubility behavior of CO_2, H_2, and Xe in imidazolium-based ILs with the $[NTf_2]^-$ anion (Andreu and Vega, 2008). The modeling of the $[C_nmim][PF_6]$ family was also extended to the description of the solubility of gases other than CO_2 and the mutual solubilities with water (Vega et al., 2010; Llovell et al., 2012a,b). Llovell et al. (2012a,b) also described NH_3, SO_2 and H_2S solubilities in three imidazolium ionic liquids families with the soft-SAFT equation of state. Oliveira et al. (2012a) used the soft-SAFT equation to describe several binary mixtures of $[C_nmim][NTf_2]$ ionic liquids surface tensions.

Even if ILs are assumed to be simple, Lennard–Jones (LJ) chains representing the ion pair, with one or multiple associating sites to account for the cation–anion interactions, soft-SAFT has been able to provide good descriptions for pure ILs properties and phase equilibria of IL containing systems using a single set of molecular parameters, most of them transferable between different ionic liquids families, and with only one or two binary interaction parameters, which are frequently temperature independent. In previous works (Andreu and Vega, 2007, 2008; Llovell et al., 2011, 2012a,b), a complete thermodynamic characterization for the imidazolium-based ILs with the anions bis(trifluoromethylsulfonyl)imide ($[NTf_2]^-$), hexafluorophosphate ($[PF_6]^-$), and tetrafluoroborate ($[BF_4]^-$) was presented, and a set of refined molecular parameters that allowed soft-SAFT EoS to be used in a semi-predictive manner was obtained for each family. Later on, the $[NTf_2]^-$ anion with the pyridinium cation family of ILs was successfully modeled (Oliveira et al., 2012b), with some of their parameters being transferred from their equivalent imidazolium-based ILs.

In this work, the ability of the soft-SAFT EoS to compute the phase equilibria of IL-based systems is extended to describe the experimental high pressure gas–liquid equilibrium (GLE) of the above mentioned gases on $[C_2mim][CH_3OHPO_2]$ by proposing new molecular models and parameters.

2. Soft-SAFT equation of state (EoS)

SAFT (Chapman et al., 1990, 1989; Huang and Radosz, 1990) was developed from a first-order approximation of the Wertheim's TPT1 perturbation theory (Wertheim, 1984a,b, 1986a,b) where the different contributions to the free energy are explicitly separated in the thermodynamic potential function. The soft-SAFT EoS (Blas and Vega, 1997) is an accurate version of SAFT, also written in terms of the sum of contributions to the total Helmholtz free energy of the system:

$$A^{rs} = A^{total} - A^{ideal} = A^{ref} + A^{chain} + A^{assoc} + A^{polar} \quad (1)$$

Each term of the above equation represents specific microscopic contributions to the total free energy (A^{total}) of the system, where A^{res} is the residual Helmholtz free energy and A^{ideal} the ideal contribution. Subsequently, A^{ref} represents the reference term expressed as the residual contributions to the free energy due to the monomer–monomer repulsive and attractive (dispersion) interactions, A^{chain} the chain formation, A^{assoc} the site–site intermolecular association and A^{polar} the polar interactions. For the soft-SAFT EoS, the reference term is a LJ spherical fluid, which takes into account the repulsive and the attractive interactions of the monomers that constitute the chain. This term includes two molecular parameters representing the monomer: the segment diameter, σ_{ii}, and the dispersive energy between segments, ε_{ii}/k_B. The reference term is

computed using the equation of Johnson et al. (1993). The extension of this term to mixtures is made by the van der Waals one-fluid theory, in which the modified Lorentz–Berthelot combining rules are applied:

$$\sigma_{ij} = \eta_{ij}\frac{\sigma_{ii}+\sigma_{jj}}{2} \tag{2}$$

$$\frac{\varepsilon_{ij}}{k_B} = \xi_{ij}\sqrt{\varepsilon_{ij}/k_B\varepsilon_{jj}/k_B} \tag{3}$$

where η_{ij} and ξ_{ij} are the size and energy binary parameters of the mixture, respectively. These values are equal to unity when using soft-SAFT EoS in a predictive manner. The chain and association terms derive from the Wertheim's TPT1 perturbation theory (Chapman et al., 1990; Huang and Radosz, 1990):

$$A^{\text{chain}} = \rho k_B T\sum_i x_i(1-m_i)\ln g_{LJ} \tag{4}$$

$$A^{\text{assoc}} = \rho k_B T\sum_i x_i\left(\sum_\alpha \ln X_i^\alpha - X_i^\alpha + \frac{M_i}{2}\right) \tag{5}$$

where ρ is the molecular density, T the temperature, m_i the chain length, x_i the molar fraction of component i,k_B the Boltzman constant and g_{LJ} the radial distribution function of a fluid at the density of the LJ spheres. g_{LJ} is fitted against computed simulation data, as function of density and temperature, as proposed by Johnson et al. (1994), $X_i{}^\alpha$ is the fraction of pure component i not bonded at site α and M_i the number of association sites of type α in component i, described as:

$$X_i^\alpha = \frac{1}{1+N_\rho\sum_j x_j\sum_\beta X_j^\beta \Delta_{\alpha\beta,ij}} \tag{6}$$

where N is the Avogadro number and $\Delta_{\alpha\beta,ij}$ the specific site–site function described as:

$$\Delta_{\alpha\beta,ij} = K^{HB}_{\alpha\beta,ij} f_{\alpha\beta,ij} g_{ij}^{LJ} \tag{7}$$

being $K^{HB}{}_{\alpha\beta,ij}$ the site–site bonding-volume of association and $\Delta_{\alpha\beta,ij}$ the Mayer f-function:

$$f_{\alpha\beta,ij} = \left[\exp\left(\frac{\varepsilon^{HB}_{\alpha\beta,ij}}{k_B T}\right) - 1\right] \tag{8}$$

The Mayer function includes the site–site association energy parameter, $\varepsilon^{HB}_{\alpha\beta,ij}$.

A multipolar term is also added for dealing with fluids of linear symmetrical molecules, like carbon dioxide, nitrogen and acetylene, for which the quadrupole–quadrupole potential must be taken into account. This term is obtained using an extension of the theory of Gubbins and Twu (1978) and the detailed description of this term can be found elsewhere (Stell et al., 1974). Two new molecular parameters are added to the model, the quadrupole moment, Q, and the fraction of segments in the chain that contains the quadrupole, x_p, as the extension of the theory to chain fluids assumes that the polar moments are well-localized on certain segments of the chain. These two parameters are correlated by the following equation:

$$Q = Q_{\text{exp}}x_p \tag{9}$$

where Q_{exp} is the experimental quadrupole moment (C m^2).

2.1. Molecular models

The key element for accurate predictions from a molecular-based EoS is the selection of a reliable coarse-grained model that can represent the basic physical features of the compound to be described, including main physical short-range interactions. The soft-SAFT EoS relies on the pre-selection of a molecular model for the pure compounds. Non-associating molecules are defined by three molecular parameters: the number of monomers forming the chain or chain length, m_i, the segment diameter, σ_{ii}, and the dispersive energy between segments, ε_{ii}/k_B. Linear symmetrical molecules usually involve two additional molecular parameters: the quadrupolar moment, Q_i, and the fraction of segments in the chain that contains the quadrupole, x_{p_i}. Finally, for associating molecules two more parameters are included to model the associating interactions: the site–site association energy, $\varepsilon^{HB}{}_{ii}/k_B$, and the site–site bonding-volume of association, $K^{\text{HB}}{}_{ii}$, while the number of associating sites and type need to be specified for each associating molecule.

The molecular parameters m_i, σ_{ii} and ε_{ii}/k_B for CO_2, CH_4 and N_2 were taken from previous works (Pàmies and Vega, 2001; Pedrosa et al., 2005). CH_4 was modeled as non-associating LJ sphere, while CO_2 and N_2 were modeled as LJ chains in which explicit quadrupolar interactions were taken into account, with x_{p_i} fixed to 1/3 and ½ respectively, representing the fraction of the chains with a quadrupole effect.

Despite molecular parameters for N_2O have been reported for PC-SAFT EoS (Arce and Aznar, 2007), this compound had never been modeled before with soft-SAFT EoS. Thus, molecular parameters for this compound were fitted in this work against its vapor-pressure and liquid density equilibrium data, taken from the NIST database (Linstrom and Mallard, 2005) in the temperature range (183–279) K, the higher temperature corresponding to a reduced temperature ($T^* = T/Tc$) of 0.9. Similar to the approach followed for the CO_2 and N_2 molecules, N_2O was modeled as a non-associating but polar compound composed by a homonuclear LJ chain in which explicit quadrupolar interactions are considered by means of an effective quadrupole moment, Q_i, contained in a certain fraction of the molecule ($x_{p_i} = 1/3$). The value of x_{p_i} mimics the N_2O molecule resonance structure with three segments with a quadrupole in one of them. The adjusted quadrupole moment is in agreement with the experimental values found in the literature (Chetty and Couling, 2011; Leung, 1998). A very good description of the equilibrium densities and vapor pressures was obtained with a percentage average absolute deviations (%AAD) of 1.54% and 3.27%. The correct soft-SAFT density and vapor pressure temperature dependencies description is depicted in Fig. S1 of Supporting Information.

In previous works (Andreu and Vega, 2007, 2008; Llovell et al., 2011; Vega et al., 2010), imidazolium-based ILs with the $[PF_6]^-$, $[BF_4]^-$ and $[NTf_2]^-$ anions were modeled either as LJ chains with one associating site, in the case of $[PF_6]^-$ and $[BF_4]^-$ ILs, or with three associating sites, for imidazolium ionic liquids containing the $[NTf_2]^-$ anion. The adopted model mimics the neutral ion pairs (anion + cation) as an LJ chain molecule with the association sites describing the specific interactions between counter-ions that result from the short range highly directional interactions coming from soften Coulomb forces, due to the bulky size and ions asymmetric charges. Dispersion forces, specific steric interactions and short-lived ion pairs also reduce the ionic character of these compounds (Weiss et al., 2010).

Here, the same approach was adopted and $[C_2\text{mim}][CH_3OHPO_2]$ was modeled as an LJ chain with two associating sites; one site A, representing the interaction of the anion oxygen with the cation, and one site B, representing the anion delocalized charge, due to the second anion oxygen atom, as represented in Fig. 1(a). Furthermore, only A–B interactions between different ILs molecules are allowed. Once the IL association scheme was selected, the molecular parameters (m_i,σ_{ii}, ε_{ii}/k_B, $\varepsilon^{\text{HB}}{}_{ii}/k_B$ and $K^{\text{HB}}{}_{ii}$) were determined by fitting them to experimental density data at atmospheric pressure (Freire et al., 2011). A very good description was obtained, as depicted in Fig. 1(b), with a %AAD of 0.65%. The higher association parameters adjusted for the $[C_2\text{mim}][CH_3OHPO_2]$, when compared to those previously

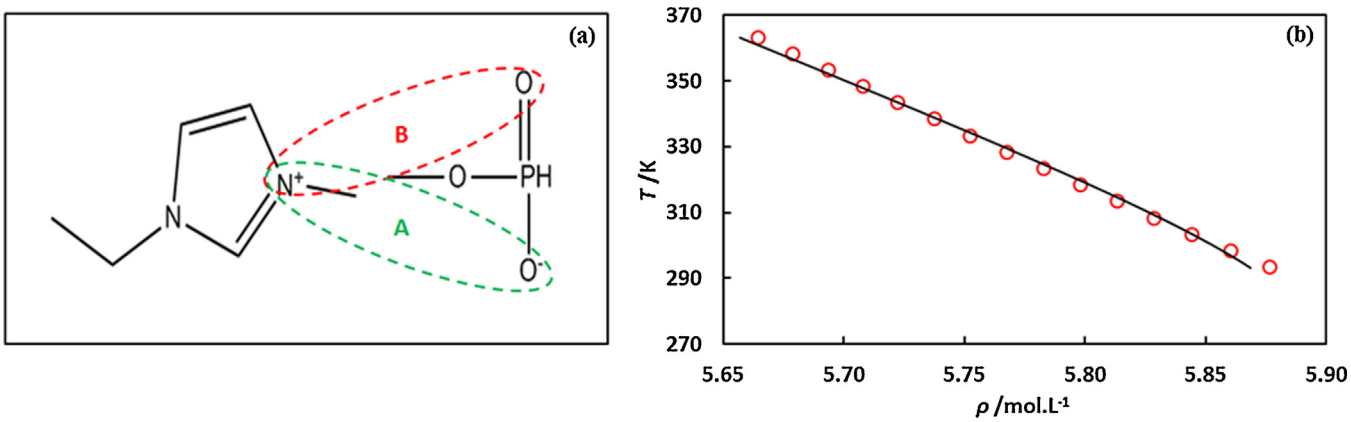

Fig. 1. (a) Scheme of association adopted for the studied IL. (b) Temperature–density diagram for the studied IL. Symbols represent experimental density data taken from the literature (Freire et al., 2011) and the solid line represents the soft-SAFT EoS fit.

reported for $[PF_6]^-$, $[BF_4]^-$ and $[NTf_2]^-$ imidazolium-based ILs (Andreu and Vega, 2007, 2008; Llovell et al., 2011) suggest higher polarity of the IL and stronger cation–anion interactions. The complete list of molecular parameters for the compounds studied is reported in Table 1.

3. Experimental

3.1. Materials

The $[C_2mim][CH_3OHPO_2]$ was obtained from Io-li-tec with mass fraction purities higher than 98%. The IL was further purified by drying under high vacuum (0.1 Pa) and moderate temperature (323 K) for a period of 48 h. The purities of the ionic liquid was checked by ^1H, ^{13}C and ^{19}P NMR before and after the purification step. The final purity is estimated to be higher than 99%. The final IL water content was determined with a Metrohm 831 Karl Fischer coulometer, indicating a water mass fraction of 97×10^{-6}.

The CO_2 and CH_4 were acquired from Air Liquide with a purity greater than 99.998% and 99.995%, respectively. The N_2O and N_2 were acquired from Praxair with a purity higher than 99.998%.

3.2. Experimental equipment

Both the apparatus and the methodology used in this work were fully described in previous works (Carvalho et al., 2009a,b,c, 2010; Mattedi et al., 2011) and shown to be adequate to accurately measure GLE in a wide range of fluids, pressures and temperatures.

The high pressure equilibrium cell is based on a cell designed by Daridon and co-workers (Dias et al., 2006; Pauly et al., 2010; Ventura et al., 2008, 2007; Vitu et al., 2008) and consists of a horizontal hollow stainless-steel cylinder, closed at one end by a movable piston and at the other end by a sapphire window, from which the operator follows the behavior of the sample with pressure (up to 100 MPa) and in the (293–363 K) temperature range.

The cell is thermostatized by circulating a heat-carrier fluid, thermo regulated using a thermostat bath circulator (Jubalo MC F25) with a temperature stability of 0.01 K, through three flow lines directly managed into the cell. The temperature inside the cell is measured by a high precision thermometer, Model PN 5207, with an uncertainty of 0.15 K connected to a calibrated platinum resistance and inserted in the cell, close to the sample. The pressure is measured by a piezoresistive silicon pressure transducer (Kulite HEM 375) fixed directly inside the cell to reduce dead volumes, which was previously calibrated and certified by an independent laboratory with IPAC accreditation, following the EN 837-1 standard and with accuracy better than 0.2%. The homogenization of the mixture is held by a small magnetic bar placed inside the cell and an external magnetic stirrer. The experimental apparatus is schematically presented in Fig. 2.

According to the applied synthetic method, a fixed amount of IL, whose exact mass is determined by weight using a high weight/high precision balance (Sartorius LA200P) with an accuracy of 1 mg, is introduced into the cell. Once introduced, the IL is kept under vacuum overnight, while stirring and heating at 353 K, in order to remove atmospheric gases absorbed during manipulation. The gas is introduced under pressure, from an ultra-lightweight composite cylinder, by means of a flexible pressure capillary and its mass measured with a high weight/high precision balance.

After preparation of a mixture with a known composition, and when the desired temperature at low pressure is reached, the pressure is then slowly increased until the system becomes monophasic. The pressure at which the last bubble disappears, for that fixed temperature and composition, represents the equilibrium pressure.

The purity of the IL is checked again by NMR at the end of the study to confirm that no degradation occurred during the measurements.

4. Results and discussions

4.1. Carbon dioxide solubility

Carbon dioxide solubility in the selected IL was measured for mole fractions ranging from (0.080 to 0.504), in the temperature range (293.23–363.34) K and pressures from (1.16 to 87.61) MPa,

Table 1
Soft-SAFT EoS molecular parameters for the compounds studied in this work.

	m_i	σ_{ii} (Å)	ε_{ii}/k_B (K)	$\varepsilon^{HB}{}_{ii}/k_B$ (K)	$K^{HB}{}_{ii}$ (Å^3)	Q_i (C m^2)	Ref.
CO_2	1.571	3.184	160.20			4.4×10^{-40}	Pedrosa et al. (2005)
N_2	1.205	3.384	89.16			1.2×10^{-40}	Pedrosa et al. (2005)
CH_4	1.000	3.728	147.20				Pàmies and Vega (2001)
N_2O	1.391	3.360	175.58			5.0×10^{-40}	This work
$[C_2mim][CH_3OHPO_2]$	5.405	3.686	414.35	4450	3950		This work

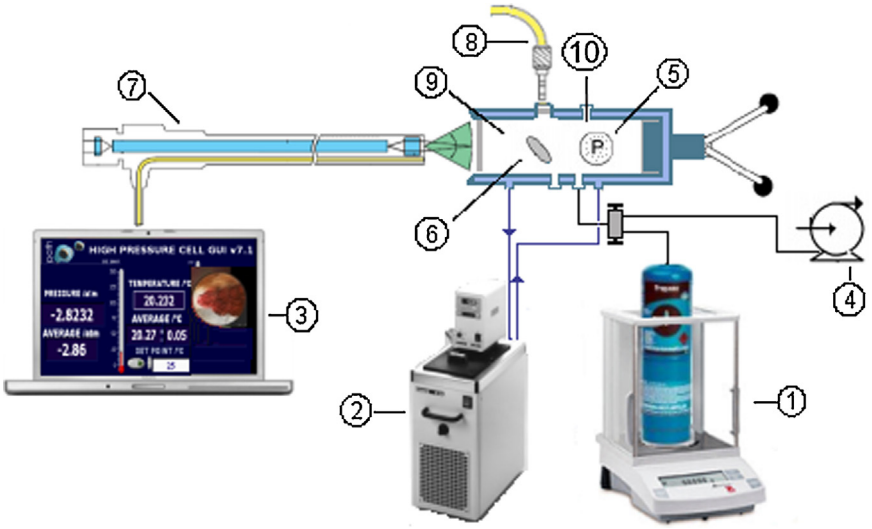

Fig. 2. Experimental apparatus schematic: 1 – Analytical balance; 2 – thermostatized bath circulator; 3 – computer to data and video acquisition; 4 – vacuum pump; 5 – piezoresistive pressure transducer; 6 – magnetic bar; 7 – endoscope plus a video camera; 8 – light source with optical fiber cable; 9 – high-pressure variable-volume cell; 10 – temperature probe.

as reported in Table S1, available in the Supporting Information, and as depicted in Fig. 3. Similar to what is observed for other ILs + CO_2 systems (Carvalho et al., 2009a,b,c,2010; Mattedi et al., 2011), the temperature increase leads to an increase on the equilibrium pressure and increasing the CO_2 concentration the equilibrium pressure increases gradually, at first, and then rapidly for higher CO_2 contents.

As depicted in Fig. 3, the soft-SAFT EoS, using one temperature dependent energy binary parameter (ξ), provides a good description of the experimental data over all the gas compositions and temperatures range. Nonetheless, the model slightly overestimates the CO_2 equilibrium pressures for a gas concentration higher than 0.40 for most isotherms and for a gas concentration higher than 0.15 for temperatures higher than 343.33 K. The binary parameter adjusted for this system follow a second order function with temperature, as depicted in Fig. S2(a) and Table S1, allowing the prediction of this parameter at other temperatures. Here, it is important to highlight that the optimized values are slightly

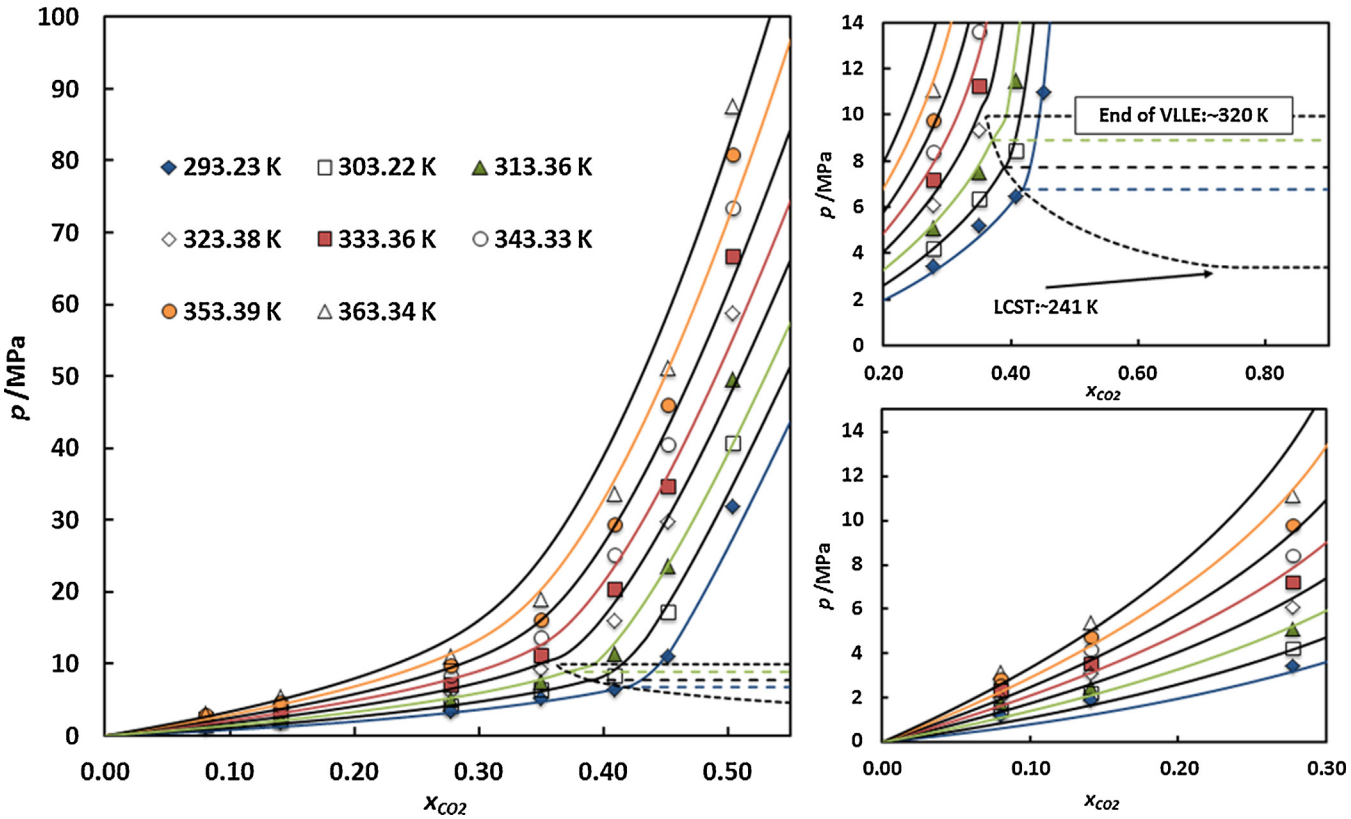

Fig. 3. Pressure-composition diagram of the binary system CO_2 + [C_2mim][CH_3OHPO_2]. The solid lines represent the soft-SAFT EoS GLE predictions and the dashed lines the VLLE description, using one temperature dependent binary parameter (ξ).

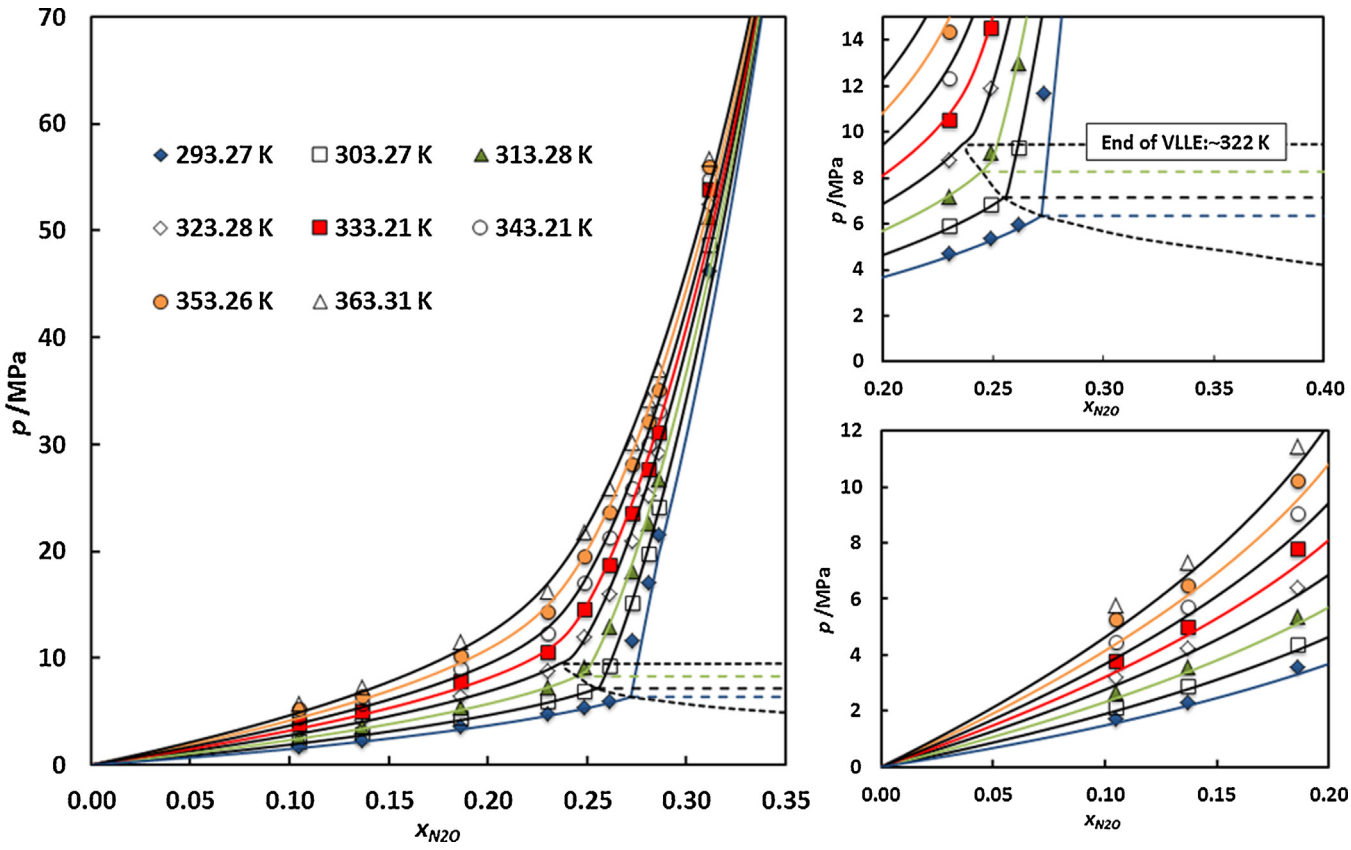

Fig. 4. Pressure-composition diagram of the binary system N_2O + [C_2mim][CH_3OHPO_2]. The solid lines represent the soft-SAFT EoS GLE predictions and the dashed lines the VLLE description, using one temperature dependent binary parameter (ξ).

over but very close to unity, indicating that the crossed dispersive energy between carbon dioxide and the IL is a bit higher than the predicted value from pure component parameters. It is also interesting to note that, as all values are very close to each other (the temperature dependence is relatively small), it is possible to describe the whole system using a constant binary parameter, despite losing a bit of accuracy in the calculations at high CO_2 concentrations (see Fig. S3). Furthermore, the soft-SAFT EoS predicts a vapor–liquid–liquid equilibrium (VLLE) for the three lowest temperatures (293.23 K, 303.22 K and 313.36 K) and for CO_2 mole fractions higher than 0.40, similar to what other authors have reported for other ILs + CO2 systems, namely the ones constituted by the ionic liquids [C_6mim][NTf_2], [C_4mim][PF_6], [C_4mim][BF_4] and [C_6mim][Ac], for which VLLE regions were predicted, using a generic cubic equations, for CO_2 mole fractions higher than 0.60 and also for the lower temperatures, between 282 and 298 K (Shiflett and Yokozeki, 2007, 2005; Shiflett et al., 2008, 2012a,b, 2011). Finally, the model predicts a liquid–liquid region with a lower critical solution temperature (LCST) at about 240 K and the end of the VLLE region at 320 K.

4.2. Nitrous oxide solubility

The solubility of nitrous oxide in [C_2mim][CH_3OHPO_2] was measured for mole fractions ranging from (0.105 to 0.312), in the temperature range (293.27–363.31) K and pressures from (1.71 to 56.75) MPa, as reported in Table S2 available in the support information, and as depicted in Fig. 4. N_2O presents similar phase equilibria behavior to that measured for CO_2, with the temperature and the N_2O concentration increase leading to higher equilibrium pressures. As for CO_2, at low N_2O concentrations the equilibrium pressure increases gradually, while it rapidly rises to higher pressures for higher N_2O contents, a typical behavior for a liquid–liquid regime. Nonetheless, the N_2O + [C_2mim][CH_3OHPO_2] reaches complete solvation much sooner than CO_2, for an N_2O mole fraction around 0.261, and afterwards the equilibrium pressure, for the studied temperatures, start to converge apparently to a crossover point that soft-SAFT predicts at an N_2O mole fraction of 0.353.

As depicted in Fig. 4, the soft-SAFT EoS provides an excellent description of the N_2O + [C_2mim][CH_3OHPO_2] system phase behavior using one temperature dependent binary parameter. The energy binary parameter (ξ) was found to follow a second order dependency with temperature as depicted in Fig. S2(b) and listed in Table S2. In this case, the binary parameter values are again very close to each other but, contrarily to the CO_2 case, they are lower than unity, indicating that the crossed dispersive energy (energetic interactions among the segments of the model) is lower than the value predicted without the correcting parameter (note that the dispersive energy value of N_2O is slightly higher than that of CO_2). Moreover, as observed for the CO_2 + [C_2mim][CH_3OHPO_2] system, the model is able to predict a liquid–liquid region and a VLLE for the three lowest temperatures (293.27, 303.27 and 313.28 K), as previously reported for other N_2O + ILs systems (Shiflett et al., 2011, 2012a,b).

4.3. Methane solubility

CH_4 solubility in [C_2mim][CH_3OHPO_2] was measured for mole fractions ranging from (0.018 to 0.054), in the temperature range (293.27–363.32) K and pressures from (2.67 to 18.02) MPa, as reported in Table S3 available in the support information, and as depicted in Fig. 5. Similar to other CH_4 + ILs systems (Carvalho and

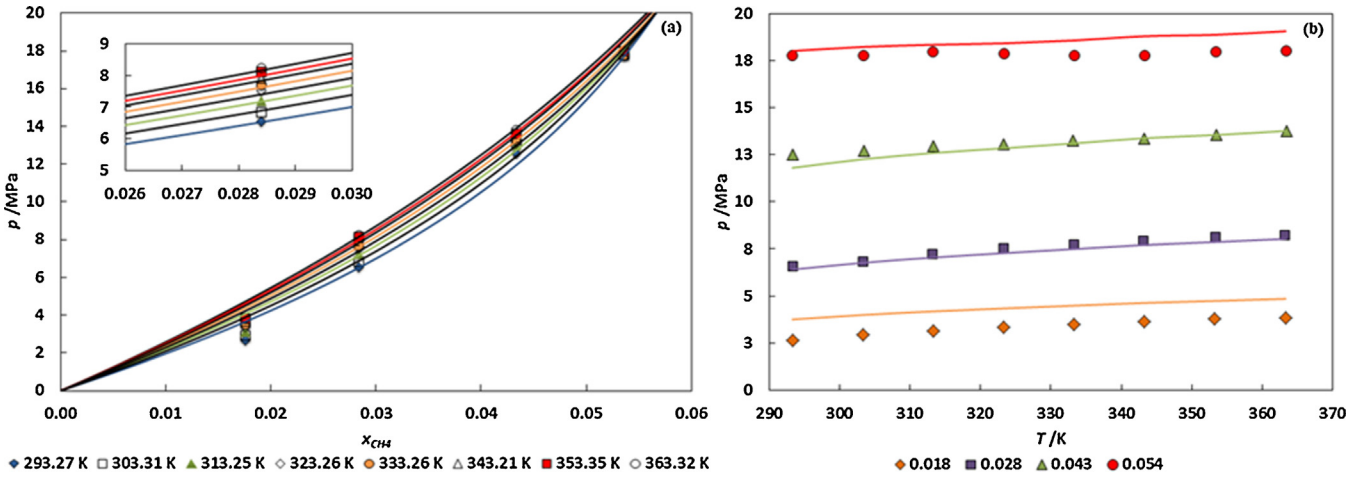

Fig. 5. (a) Pressure-composition and (b) pressure–temperature diagrams for the binary system CH_4 + [C_2mim][CH_3OHPO_2]. The solid lines represent the soft-SAFT EoS GLE description with one temperature dependent binary parameter (η).

Coutinho, 2011), the temperature has a very small impact on the CH_4 solubility. Despite this small temperature dependence, soft-SAFT EoS provides a good description of the experimental data, as depicted in Fig. 5, using a size binary parameter (η) that takes in consideration the strong influence of the size difference between the segments forming the two compounds. In this case, the energy parameter does not have an important impact, as the crossed-energy interactions between methane and the IL are expected to be relatively small. The adjusted binary parameters are reported in Table S3 and depicted in Fig. S2(c) available in the support information, and follow a second order dependence with temperature. Once again, the binary parameter values are very similar and, in this case, higher than unity, suggesting a high degree of entropy in the system (the segment diameter of the mixture is higher than the average of the segment diameter of each compound separately). Furthermore, and as reported before for other polar ILs (Carvalho and Coutinho, 2011), CH_4 has a very low solubility in [C_2mim][CH_3OHPO_2] when compared with the other gases studied.

4.4. Nitrogen solubility

The solubility of nitrogen in [C_2mim][CH_3OHPO_2] was measured for mole fractions ranging from (0.017 to 0.044), in the temperature range (293.31 to 363.33) K and pressures from (14.33 to 89.43) MPa, as reported in Table S4, available in the support information, and as depicted in Fig. 5. Contrary to what was observed for the other systems studied in this work, a temperature increase leads to a decrease of the equilibrium pressure. This behavior, although quite remarkable, is not unique and it has been previously reported for N_2 solubilities in alkanes (Eliosa-Jiménez et al., 2009; Lin et al., 1981; Silva-Oliver et al., 2007, 2006). Moreover, similar reverse dependencies of the solubility with temperature have been reported for CH_4 + ILs (Carvalho and Coutinho, 2011) and for H_2 + ILs systems (Kumełan et al., 2006a,b). The reasons behind this phenomenon are not yet fully understood but a possible explanation can be that the N_2 + [C_2mim][CH_3OHPO_2] system is also characterized by a type III phase diagram, according to the classification of Konynenburg and Van Scott (1980), as observed for the N_2+ alkanes systems (Eliosa-Jiménez et al., 2009; Lin et al., 1981; Silva-Oliver et al., 2007, 2006), although further investigations are needed to corroborate this claim.

Nitrogen presents a very low solubility in the IL, which is even lower than the one measured for CH_4. As an example, a pressure of approximately 90 MPa is required in order to solubilize an N_2 mole fraction of 0.044 at 293.31 K, while a pressure of approximately 13 MPa is required to solubilize a similar amount of CH_4.

The thermodynamic modeling of the system with soft-SAFT is able to reproduce this inverse trend of the solubility with the temperature using an energy binary parameter (ξ) with a second order dependence with temperature (Table S4 and Fig. S2(d) in the support information section). Unfortunately, despite successfully describing the system phase behavior for N_2 mole fractions up to 0.035, as depicted in Fig. 6(b), the soft-SAFT EoS is not able to describe the change on the GLE behavior, as it can be observed in Fig. 6(a). As a consequence, an over-prediction of the equilibrium pressure for the two highest concentrations (0.040 and 0.044) occurs, as seen in Fig. 6(b).

4.5. Henry's constant and selectivities

The Henry's law relates the amount of a given gas dissolved in a liquid, at a constant temperature, to the fugacity of that gas in equilibrium with that liquid and can be described as:

$$H_{i,L}(T,p) = \lim_{x_i \to 0} \frac{f_i^L}{x_i} \tag{10}$$

where $H_{i,L}(T,p)$ is the Henry's constant, x_i is the mole fraction of gas i dissolved in the liquid, and f_i^L is the fugacity of the gas i in the liquid phase (L). As shown, Eq. (10) is only rigorously valid in the diluted region limit. In this work, the Henry's constants were estimated by fitting the soft-SAFT EoS to the experimental data and calculating the limiting slope as the solubility approaches zero.

Although this procedure introduces some uncertainty on the estimated Henry's constants, the results obtained for the gases are different enough to allow a discussion on the solvation of the gases on the IL. Henry's constants for the gas + [C_2mim][CH_3OHPO_2] binary systems as a function of temperature are reported in Supporting Information, Table 2.

The Henry's constant for the studied gases in [C_2mim][CH_3OHPO_2], at a selected temperature of 313 K, are reported in Table 3 along with the Henry's constants of these gases on other ILs, such as 1-ethyl-3-methylimidazolium tetrafluoroborate ([C_2mim][BF_4]), 1-ethyl-3-methylimidazolium dicyanamide ([C_2mim][$N(CN)_2$]) and 1-ethyl-3-methylimidazolium bis(trifluoromethylsulfonyl)imide ([C_2mim][NTf_2]). Data for other solvents commonly used for CO_2 capture, such as triethylene glycol monomethyl ether (TEGMME), methanol (CH_3OH) and

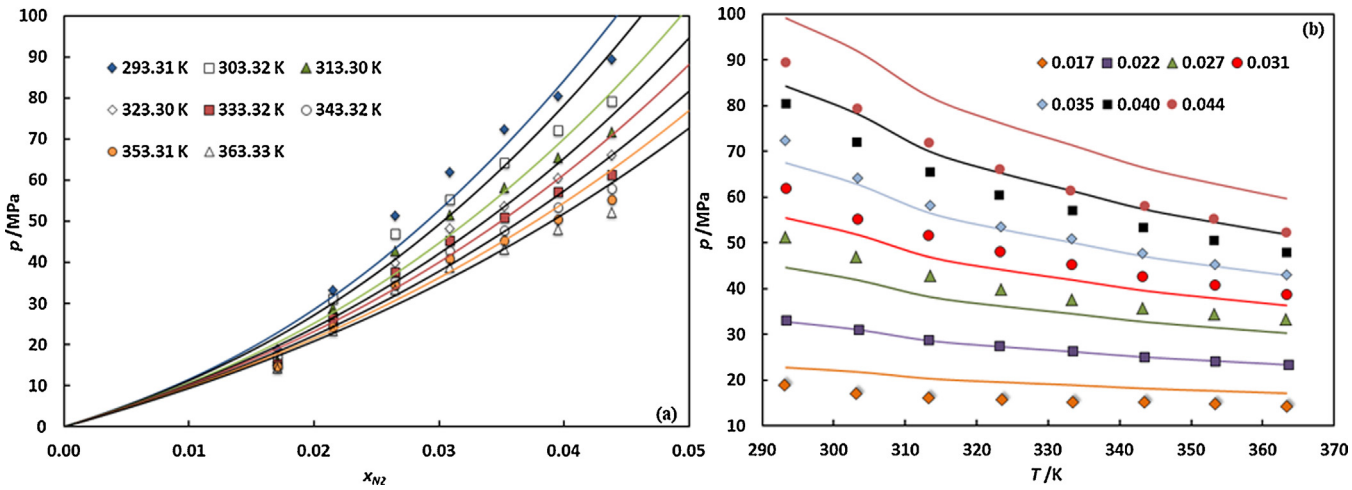

Fig. 6. (a) Pressure-composition and (b) pressure–temperature diagrams for the binary system N_2 + [C_2mim][CH_3OHPO_2]. The solid lines represent the soft-SAFT EoS GLE description with one temperature dependent binary parameter (ξ).

Table 2
Estimated Henry's law constants (MPa) for CO_2, N_2O, CH_4 and N_2 in [C_2mim][CH_3OHPO_2].

	293.15 K	303.15 K	313.15 K	323.15 K	333.15 K	343.15 K	353.15 K	363.15 K
CO_2	6.75	9.48	12.32	15.44	18.58	21.99	25.71	29.49
N_2O	12.38	16.10	19.90	23.80	27.72	32.62	35.53	39.57
CH_4	184.40	197.25	207.73	216.68	225.10	233.06	239.33	245.84
N_2	966.00	959.62	927.87	913.50	902.29	882.91	870.78	855.85

aqueous solutions of MEA (40%), i.e., at 40 wt%, are also included for comparison. MEA is a solvent widely used as chemical absorption solvent in the capture of CO_2, while CH_3OH and TEGMME are used as physical solvents in the reduction of this pollutant (Olajire, 2010; Henni and Mather, 1995a,b,c).

As shown in Table 3, the IL studied in this work presents slightly higher carbon dioxide and methane Henry's constants, i.e. lower solubilities, than the remaining ILs. Interestingly, the nitrogen Henry's constant for [C_2mim][CH_3OHPO_2] is much higher than those reported for all the other solvents.

The selection of a solvent for an efficient separation process must focus on the choice of a highly selective solvent. Previously, Carvalho and Coutinho (2010b) have shown that the CO_2 solubility in ionic liquids is controlled by entropic effects and that it is similar for a large number of ionic liquids and thus, the maximization of the selectivity must address the minimization of the other gas (N_2, CH_4) solubilities in the ionic liquid. Since, and unlike the CO_2, the solubility of CH_4 and N_2 in ionic liquids is controlled by the unfavorable interactions between the gas and the solvent (Carvalho and Coutinho, 2011), the IL that will maximize the non-ideality of the liquid phase will also minimize the gas solubility and thus maximize the selectivity. Following the approach proposed in previous work (Carvalho and Coutinho, 2011), the ideal gas selectivity ($S_{1/2}$) was determined for the four gases studied through its Henry's constants:

$$S_{1/2} = \frac{H_{2,L}}{H_{1,L}} \tag{11}$$

where $H_{i,L}$ stands for the Henry's constant of gas i.

The results show that the solubility of nitrogen is very low in most ILs (high Henry's constant), and therefore an exceptional selectivity toward greenhouse gases can be achieved when compared to traditional solvents. This results make the highly polar [C_2mim][CH_3OHPO_2] the best suitable IL for carbon dioxide and methane capture and only slightly below [C_2mim][$N(CN)_2$] and [C_2mim][BF_4] for nitrous oxide capture, within the studied ILs.

Although the highly polar [C_2mim][CH_3OHPO_2] presents very low nitrogen solubility, and therefore very high CO_2/N_2 and N_2O/N_2 selectivities, the methane solubility is higher than expected. Moreover, the carbon dioxide solubility is also lower than that reported for other size-equivalent ILs. Thus, the mechanism behind the sorption of carbon dioxide, methane and nitrogen in other phosphonate-based ILs (1,3-dimethylimidazolium methyl-phosphonate [C_1mim][CH_3OHPO_2], 1-butyl-3-methylimidazolium methyl-phosphonate [C_4mim][CH_3OHPO_2], 1-ethyl-3-methylimidazolium ethyl-phosphonate [C_2mim][$C_2H_5OHPO_2$],

Table 3
Estimated and reported Henry's constants (MPa) and selectivity for the selected gases in ILs and some common solvents at 313 K.

	H_{CO_2}	H_{N_2O}	H_{CH_4}	H_{N_2}	S_{CO_2/N_2}	S_{CO_2/N_2}	S_{CH_4/N_2}	S_{CO_2/CH_4}	Ref
[C_2mim][CH_3OHPO_2]	12.32	19.90	207.73	927.87	75.31	46.63	4.47	16.86	This work
[C_2mim][BF_4]	10.13		202.70	385.00	38.01	48.98[a]	1.90	20.01	Finotello et al. (2008)
[C_2mim][$N(CN)_2$]	9.73		202.70	496.50	51.03	57.13[a]	2.45	20.83	Camper et al. (2006)
[C_2mim][NTf_2]	5.07		56.74	121.60	23.98	37.88[a]	2.14	11.19	Finotello et al. (2008)
MEA (40%)					25.67[b]			7.70[b]	Xu et al. (2009)
CH_3OH	15.60		112.32	358.80	23.00		3.19	7.20	Lin and Freeman (2005)
TEGMME	7.50	8.10	85.03					11.34	Henni and Mather (1995a,b,c)

[a] Estimated using the N_2O Henry's constants reported for the analogous [C_4mim] at 298.15 K (Shiflett et al., 2012a,b).
[b] Values taken from the study of the absorption of CO_2, N_2 and CH_4 in MEA (40%) fixed in β-zeolite (Xu et al., 2009).

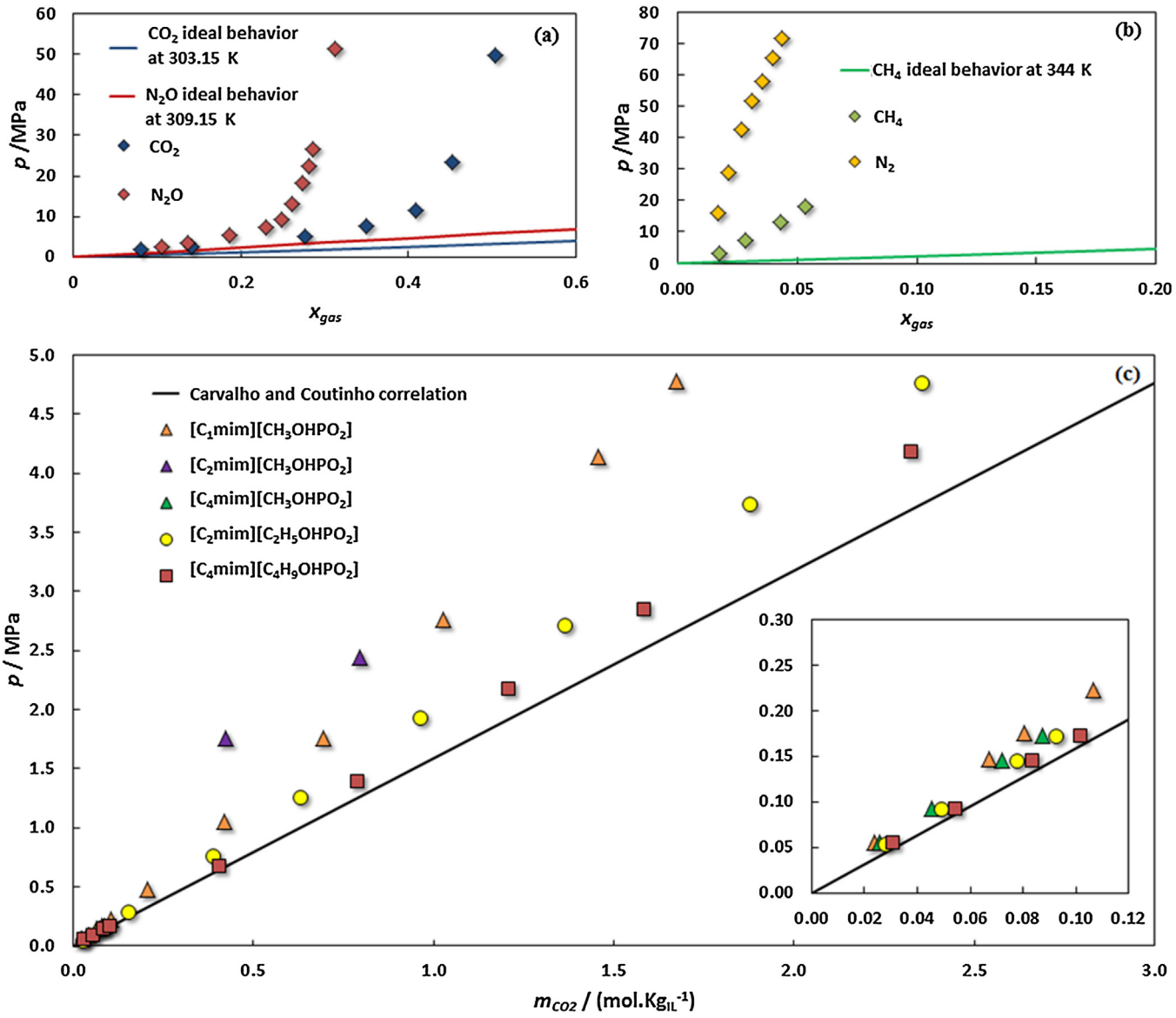

Fig. 7. Pressure-composition diagrams for the binary systems: (a) CO_2 *and* N_2O + $[C_2mim][CH_3OHPO_2]$, (b) CH_4 and N_2 + $[C_2mim][CH_3OHPO_2]$ and (c) pressure-molality diagrams for the binary systems CO_2 + phosphonate-based ILs at 313 K (Palgunadi et al., 2009). The solid lines represent (a) the Raoult's law for CO_2 at 303.15 K and N_2O at 309.15 K, (b) the binary system CH_4 + hexane (Poston and McKetta, 1966) at 310.93 K and (c) the universal correlation proposed in previous work at 313.15 K (Carvalho and Coutinho, 2010a).

1-butyl-3-methylimidazolium buthyl-phosphonate $[C_4mim][C_4H_9OHPO_2]$) was also investigated by analyzing their deviations from ideality in the liquid phase (Palgunadi et al., 2009). The system CH_4 + hexane (Poston and McKetta, 1966), an athermic, quasi-ideal mixture, with negligible enthalpic interactions and reduced entropic contributions resulting from the differences in size and shape of the involved species, was adopted to describe the methane ideal behavior, while the extended Raoult's law was used to describe CO_2 and N_2O.

Fig. 7 shows a peculiar behavior with both the $[C_2mim][CH_3OHPO_2]$ + CO_2 and $[C_2mim][CH_3OHPO_2]$ + N_2O binary systems presenting positive deviations to ideality. Furthermore, this peculiar behavior is common to the other phosphonate-based ILs evaluated and supports the low solubilities and high selectivities obtained. Moreover, even if the molecular weight is removed from the analysis, by comparing the solubilities in molalities instead of molar fractions, the CO_2 solubility still presents higher equilibrium pressures than those predicted by the correlation previously proposed for CO_2 + non-volatile solvents (Carvalho and Coutinho, 2010a). The results apparently suggest that highly polar ionic liquids present unfavorable interactions toward the studied gases and that, if one targets a highly selective solvent for CO_2/N_2 or CO_2/CH_4 separation, a delicate balance between the solvent polarity (Carvalho and Coutinho, 2011) and molar volume (Scovazzo, 2009) must be ascertained. On the contrary, the methane and nitrogen present the expected strong positive deviations to ideality, already observed for other systems (Carvalho and Coutinho, 2011), which are favorable to achieve high selectivities.

5. Conclusions

Understanding the solubility of gases in ILs in a wide range of molar fractions, temperatures and pressures is essential for the adequate development and optimization of ionic liquid based process for high pressure capture of greenhouse gases. In this work, new gas–liquid equilibrium data for CO_2, N_2O, N_2 and CH_4 in 1-ethyl-3-methylimidazolium methyl-phosphonate have been measured in the temperature range (293–363) K and pressures

ranging from (1 to 89) MPa. A highly polar ionic liquid was selected giving new insights about the gases–ILs interactions.

The highly polar [C_2mim][CH_3OHPO_2] presents low N_2 solubility and the highest CO_2/N_2 selectivity reported for ILs. Nonetheless, both CH_4 and CO_2 present lower solubilities than expected, with the later presenting positive deviations to ideality. This unusual behavior, here reported for the first time, indicates that highly polar ionic liquids present unfavorable interactions toward the studied gases and that if one targets a highly selective solvent for CO_2/N_2 or CO_2/CH_4 separation a delicate balance between the solvent polarity and its molar volume must be ascertained.

The soft-SAFT EoS was used to describe the high pressure phase behavior. A new molecular model for N_2O and [C_2mim][CH_3OHPO_2] was proposed. The quadrupole moment of N_2O was explicitly considered, while the ion pair assumption with two sites to represent the cation–anion interactions was used for the IL. The model allowed a good description of both, the pure fluids and all the studied binary systems, and was able to reproduce the small CH_4 temperature dependency and the N_2 reverse temperature dependency on the solubility using only one binary parameter. Using no more than one and temperature independent binary interaction parameter, the soft-SAFT stands as a powerful tool to be applied in the development and optimization of high pressure capture of greenhouse gases processes using ionic liquids, when experimental data is not available.

Aiming to fully understand the sorption mechanism responsible for the solubility of gases in ILs, further steps will be devoted to the extension of this type of experimental measurements and modeling approaches to systems composed of different ionic liquids and other hazardous air pollutants.

Acknowledgments

The authors are thankful for financial support from Fundação para a Ciência e a Tecnologia (Project PTDC/EQU-FTT/102166/2008), Laboratório Associado Centro de Investigação em Materiais Cerâmicos e Compósitos (Project Pest-C/CTM/LA0011/2013), Post-Doctoral grants of Pedro J. Carvalho (SFRH/BPD/82264/2011), Mariana B. Oliveira (SFRH/BPD/71200/2010) and Ana M.A. Dias (SFRH/BPD/40409/2007). F. Llovell acknowledges a TALENT contract from the Catalan Government. Additional financial support was provided by the Spanish government, Ministerio de Economía y Competitividad (projects CTQ2008-05370/PPQ and CENIT SOST-CO2 CEN2008-01027) and the Catalan government (project 2009SGR-666). Support from Carburos Metálicos, Air Products Group, is also acknowledged.

Appendix A. Supplementary data

Supplementary material related to this article can be found, in the online version, at doi:10.1016/j.ijggc.2013.09.007.

References

Andreu, J., Vega, L., 2007. Capturing the solubility behavior of CO2 in ionic liquids by a simple model. Journal of Physical Chemistry C 111, 16028–16034.

Andreu, J.S., Vega, L.F., 2008. Modeling the solubility behavior of CO2, H2, and Xe in [Cn-mim][Tf2N] ionic liquids. Journal of Physical Chemistry B 112, 15398–15406.

Arce, P., Aznar, M., 2007. Modeling of critical lines and regions for binary and ternary mixtures using non-cubic and cubic equations of state. Journal of Supercritical Fluids 42, 1–26.

Bara, J.E., Carlisle, T.K., Gabriel, C.J., Camper, D., Finotello, A., Gin, D.L., Noble, R.D., 2009. Guide to CO2 separations in imidazolium-based room-temperature ionic liquids. Industrial & Engineering Chemistry Research 48, 2739–2751.

Blas, F.J., Vega, L.F., 1997. Thermodynamic behaviour of homonuclear and heteronuclear Lennard-Jones chains with association sites from simulation and theory. Molecular Physics 92, 135–150.

Camper, D., Bara, J., Koval, C., Noble, R., 2006. Bulk-fluid solubility and membrane feasibility of Rmim-based room-temperature ionic liquids. Industrial & Engineering Chemistry Research 45, 6279–6283.

Carvalho, P.J., Coutinho, J.A.P., 2010a. On the nonideality of CO2 solutions in ionic liquids and other low volatile solvents. Journal of Physical Chemistry Letters 1, 774–780.

Carvalho, P.J., Coutinho, J.A.P., 2010b. Non-ideality of solutions of NH3 SO2, and H2 S in ionic liquids and the prediction of their solubilities using the Flory Huggins model. Energy & Fuels 24, 6662–6666.

Carvalho, P.J., Coutinho, J.A.P., 2011. The polarity effect upon the methane solubility in ionic liquids: a contribution for the design of ionic liquids for enhanced CO2/CH4 and H2S/CH4 selectivities. Energy & Environmental Science 4, 4614–4619.

Carvalho, P.J., Álvarez, V.H., Machado, J.J.B., Pauly, J., Daridon, J.-L., Marrucho, I.M., Aznar, M., Coutinho, J.A.P., 2009a. High pressure phase behavior of carbon dioxide in 1-alkyl-3-methylimidazolium bis(trifluoromethylsulfonyl)imide ionic liquids. Journal of Supercritical Fluids 48, 99–107.

Carvalho, P.J., Álvarez, V.H., Marrucho, I.M., Aznar, M., Coutinho, J.A.P., 2009b. High pressure phase behavior of carbon dioxide in 1-butyl-3-methylimidazolium bis(trifluoromethylsulfonyl)imide and 1-butyl-3-methylimidazolium dicyanamide ionic liquids. Journal of Supercritical Fluids 50, 105–111.

Carvalho, P.J., Alvarez, V.H., Schröder, B., Gil, A.M., Marrucho, I.M., Aznar, M., Santos, L.M.N.B.F., Coutinho, J.A.P., 2009c. Specific solvation interactions of CO2 on acetate and trifluoroacetate imidazolium based ionic liquids at high pressures. Journal of Physical Chemistry B 113, 6803–6812.

Carvalho, P.J., Álvarez, V.H., Marrucho, I.M., Aznar, M., Coutinho, J.A.P., 2010. High carbon dioxide solubilities in trihexyltetradecylphosphonium-based ionic liquids. Journal of Supercritical Fluids 52, 258–265.

Chapman, W.G., Gubbins, K.E., Jackson, G., Radosz, M., 1989. SAFT: equation-of-state solution model for associating fluids. Fluid Phase Equilibria 52, 31–38.

Chapman, W.G., Gubbins, K.E., Jackson, G., Radosz, M., 1990. New reference equation of state for associating liquids. Industrial & Engineering Chemistry Research 29, 1709–1721.

Chen, Y., Mutelet, F., Jaubert, J.N., 2012. Modeling the solubility of carbon dioxide in imidazolium based ionic liquids with the PC-SAFT equation of state. Journal of Physical Chemistry B 116, 14375–14388.

Chetty, N., Couling, V.W., 2011. Measurement of the electric quadrupole moment of N2O. Journal of Chemical Physics 134, 144307.

Chiappe, C., Pieraccini, D., 2005. Ionic liquids: solvent properties and organic reactivity. Journal of Physical Organic Chemistry 18, 275–297.

Dias, A.M.A., Carrier, H., Daridon, J.L., Pàmies, J.C., Vega, L.F., Coutinho, J.A.P., Marrucho, I.M., 2006. Vapor-liquid equilibrium of carbon dioxide-perfluoroalkane mixtures: experimental data and SAFT modeling. Industrial & Engineering Chemistry Research 45, 2341–2350.

Eliosa-Jiménez, G., García-Sánchez, F., Silva-Oliver, G., Macías-Salinas, R., 2009. Vapor–liquid equilibrium data for the nitrogen + n-octane system from (344.5 to 543.5) K and at pressures up to 50 MPa. Fluid Phase Equilibria 282, 3–10.

Ferguson, L., Scovazzo, P., 2007. Solubility, diffusivity and permeability of gases in phosphonium-based room temperature ionic liquids: data and correlations. Industrial & Engineering Chemistry Research 46, 1369–1374.

Finotello, A., Bara, J.E., Camper, D., Noble, R.D., 2008. Room-temperature ionic liquids: temperature dependence of gas solubility selectivity. Industrial & Engineering Chemistry Research 47, 3453–3459.

Freire, M.G., Teles, A.R.R., Rocha, M.A.A., Schröder, B., Neves, C.M.S.S., Carvalho, P.J., Evtuguin, D.V., Santos, L.M.N.B.F., Coutinho, J.A.P., 2011. Thermophysical characterization of ionic liquids able to dissolve biomass. Journal of Chemical & Engineering Data 56, 4813–4822.

Gubbins, K.E., Twu, C.H., 1978. Thermodynamics of polyatomic fluid mixtures – I theory. Chemical Engineering Science 33, 863–878.

Henni, A., Mather, A., 1995a. Solubility of nitrous oxide in triethylene glycol monomethyl ether at elevated pressures. Journal of Chemical & Engineering Data Engineering Data 40, 1158–1160.

Henni, A., Mather, A.E., 1995b. The solubility of CO2 in triethylene glycol monomethyl ether. Canadian Journal of Chemical Engineering 73, 156–158.

Henni, A., Mather, A.E., 1995c. The solubility of methane in triethylene glycol monomethyl ether. Fluid Phase Equilibria 108, 213–218.

Huang, S.H., Radosz, M., 1990. Equation of state for small, large, polydisperse, and associating molecules. Industrial & Engineering Chemistry Research 29, 2284–2294.

IPCC, 2007. Climate change 2007: Synthesis Report. Intergovernmental Panel on Climate Change (IPCC).

Ji, X., Adidharma, H., 2009. Thermodynamic modeling of ionic liquid density with heterosegmented statistical associating fluid theory. Chemical Engineering Science 64, 1985–1992.

Ji, X., Adidharma, H., 2010. Thermodynamic modeling of CO2 solubility in ionic liquid with heterosegmented statistical associating fluid theory. Fluid Phase Equilibria 293, 141–150.

Johnson, J.K., Zollweg, J., Gubbins, K.E.a., 1993. The Lennard-Jones equation of state revisited. Molecular Physics 78, 591–618.

Johnson, J.K., Mueller, E.A., Gubbins, K.E., 1994. Equation of State for Lennard-Jones Chains. Journal of Physical Chemistry 98, 6413–6419.

Karakatsani, E.K., Economou, I.G., Kroon, M.C., Peters, C.J., Witkamp, G.-J., 2007. tPC-PSAFT modeling of gas solubility in imidazolium-based ionic liquids. Journal of Physical Chemistry C 111, 15487–15492.

Konynenburg, P.H., Van Scott, R.L., 1980. Critical lines and phase equilibria in binary Van Der Waals mixtures. Philosophical Transactions of the Royal

Society of London. Series A, Mathematical and Physical Sciences 298, 495–540.
Kroon, M.C., Karakatsani, E.K., Economou, I.G., Witkamp, G.-J., Peters, C.J., 2006. Modeling of the carbon dioxide solubility in imidazolium-based ionic liquids with the tPC-PSAFT equation of state. Journal of Physical Chemistry B 110, 9262–9269.
Kumełan, J., Pérez-Salado Kamps, Á., Tuma, D., Maurer, G., 2006a. Solubility of H2 in the ionic liquid [bmim][PF6]. Journal of Chemical & Engineering Data 51, 11–14.
Kumełan, J., Pérez-Salado Kamps, Á., Tuma, D., Maurer, G., 2006b. Solubility of H2 in the ionic liquid [hmim][Tf2N]. Journal of Chemical & Engineering Data 51, 1364–1367.
Leung, H.O., 1998. The rotational spectrum and nuclear quadrupole hyperfine structure of CO2–N2O. Journal of Chemical Physics 108, 3955.
Lin, H., Freeman, B.D., 2005. Materials selection guidelines for membranes that remove CO2 from gas mixtures. Journal of Molecular Structure 739, 57–74.
Lin, H.-M., Kim, H., Chao, K.-C., 1981. Gas–liquid equilibria in nitrogen + n-hexadecane mixtures at elevated temperatures and pressures. Fluid Phase Equilibria 7, 181–185.
Linstrom, P.J., Mallard, W.G., 2005. NIST Chemistry WebBook, NIST Standard Reference Database Number 69. National Institute of Standards and Technology, Gaithersburg, MD, pp. 20899 (http://webbook.nist.gov). June.
Llovell, F., Valente, E., Vilaseca, O., Vega, L.F., 2011. Modeling complex associating mixtures with [Cn-mim][Tf2N] ionic liquids: predictions from the soft-SAFT equation. Journal of Physical Chemistry B 115, 4387–4398.
Llovell, F., Marcos, R.M., MacDowell, N., Vega, L.F., 2012a. Modeling the absorption of weak electrolytes and acid gases with ionic liquids using the soft-SAFT approach. Journal of Physical Chemistry B 116, 7709–7718.
Llovell, F., Vilaseca, O., Vega, L.F., 2012b. Thermodynamic modeling of imidazolium-based ionic liquids with the [PF6]- anion for separation purposes. Separation Science and Technology 47, 399–410.
Marsh, K.N., Boxall, J.A., Lichtenthaler, R., 2004. Room temperature ionic liquids and their mixtures—a review. Fluid Phase Equilibria 219, 93–98.
Mattedi, S., Carvalho, P.J., Coutinho, J.A.P., Alvarez, V.H., Iglesias, M., 2011. High pressure CO2 solubility in N-methyl-2-hydroxyethylammonium protic ionic liquids. Journal of Supercritical Fluids 56, 224–230.
Morgan, D., Ferguson, L., Scovazzo, P., 2005. Diffusivities of gases in room-temperature ionic liquids: data and correlations obtained using a Lag-Time technique. Industrial & Engineering Chemistry Research 44, 4815–4823.
Olajire, A.A., 2010. CO2 capture and separation technologies for end-of-pipe applications – a review. Energy 35, 2610–2628.
Oliveira, M.B., Domínguez-Pérez, M., Freire, M.G., Llovell, F., Cabeza, O., Lopes-da-Silva, J.A., Vega, L.F., Coutinho, J.A.P., 2012a. Surface tension of binary mixtures of 1-alkyl-3-methylimidazolium bis(trifluoromethylsulfonyl)imide ionic liquids: experimental measurements and soft-SAFT modeling. Journal of Physical Chemistry B 116, 12133–12141.
Oliveira, M.B., Llovell, F., Coutinho, J.aP., Vega, L.F., 2012b. Modeling the [NTf2] pyridinium ionic liquids family and their mixtures with the soft statistical associating fluid theory equation of state. Journal of Physical Chemistry B 116, 9089–9100.
Palgunadi, J., Kang, J.E., Cheong, M., Kim, H., Lee, H., Kim, H.S., 2009. Fluorine-free imidazolium-based ionic liquids with a phosphorous-containing anion as potential CO2 absorbents. Bulletin of the Korean Chemical Society 30, 1749–1754.
Pàmies, J., Vega, L., 2001. Vapor–liquid equilibria and critical behavior of heavy n-alkanes using transferable parameters from the soft-SAFT equation of state. Industrial & Engineering Chemistry Research 40, 2532–2543.
Pauly, J., Coutinho, J.A.P., Daridon, J.-L., 2010. High pressure phase equilibria in methane + waxy systems, 2. Methane + waxy ternary mixture. Fluid Phase Equilibria 297, 149–153.
Pedrosa, N., Pàmies, J.C., Coutinho, J.A.P., Marrucho, I.M., Vega, L.F., 2005. Phase equilibria of ethylene glycol oligomers and their mixtures. Industrial & Engineering Chemistry Research 44, 7027–7037.
Poloncarzova, M., Vejrazka, J., Vesely, V., Izak, P., 2011. Effective purification of biogas by a condensing-liquid membrane. Angewandte Chemie 50, 669–671 (International Ed. in English).
Poston, R.S., McKetta, J.J., 1966. Vapor–liquid equilibrium in the methane-n-hexane system. Journal of Chemical & Engineering Data 11, 362–363.
Ravishankara, A.R., Daniel, J.S., Portmann, R.W., 2009. Nitrous oxide (N2O): the dominant ozone-depleting substance emitted in the 21st century. Science 326, 123–125.
Revelli, A.-L., Mutelet, F., Jaubert, J.-N., 2010a. Reducing of nitrous oxide emissions using ionic liquids. Journal of Physical Chemistry B 114, 8199–8206.
Revelli, A.-L., Mutelet, F., Jaubert, J.-N., 2010b. High carbon dioxide solubilities in imidazolium-based ionic liquids and in poly(ethylene glycol) dimethyl ether. Journal of Physical Chemistry B 114, 12908–12913.
Rogers, R.D., Seddon, K.R., 2003. Ionic liquids – solvents of the future? Science 302, 792–793.
Scovazzo, P., 2009. Determination of the upper limits, benchmarks, and critical properties for gas separations using stabilized room temperature ionic liquid membranes (SILMs) for the purpose of guiding future research. Journal of Membrane Science 343, 199–211.
Scovazzo, P., Havard, D., McShea, M., Mixon, S., Morgan, D., 2009. Long-term, continuous mixed-gas dry fed CO2/CH4 and CO2/N2 separation performance and selectivities for room temperature ionic liquid membranes. Journal of Membrane Science 327, 41–48.
Shiflett, M.B., Yokozeki, A., 2005. Solubilities and diffusivities of carbon dioxide in ionic liquids: [bmim][PF6] and [bmim][BF4]. Industrial & Engineering Chemistry Research 44, 4453–4464.
Shiflett, M.B., Yokozeki, A., 2007. Solubility of CO2 in room temperature ionic liquid [hmim][Tf2N]. Journal of Physical Chemistry B 111, 2070–2074.
Shiflett, M.B., Kasprzak, D.J., Junk, C.P., Yokozeki, A., 2008. Phase behavior of {carbon dioxide + [bmim][Ac]} mixtures. Journal of Chemical Thermodynamics 40, 25–31.
Shiflett, M.B., Drew, D.W., Cantini, R.A., Yokozeki, A., 2010. Carbon dioxide capture using ionic liquid 1-butyl-3-methylimidazolium acetate. Energy & Fuels 24, 5781–5789.
Shiflett, M.B., Niehaus, A.M.S., Yokozeki, A., 2011. Separation of N2O and CO2 using room-temperature ionic liquid [bmim][BF4]. Journal of Physical Chemistry B 115, 3478–3487.
Shiflett, M.B., Elliott, B.A., Niehaus, A.M.S., Yokozeki, A., 2012a. Separation of N2O and CO using room-temperature ionic liquid [bmim][Ac]. Separation Science and Technology 47, 411–421.
Shiflett, M.B., Niehaus, A.M.S., Elliott, B.A., Yokozeki, A., 2012b. Phase behavior of N2O and CO2 in room-temperature ionic liquids [bmim][Tf2 N], [bmim][BF4], [bmim][N(CN)2], [bmim][Ac], [eam][NO3], and [bmim][SCN]. International Journal of Thermophysics 33, 412–436.
Silva-Oliver, G., Eliosa-Jiménez, G., García-Sánchez, F., Avendaño-Gómez, J.R., 2006. High-pressure vapor–liquid equilibria in the nitrogen – n-pentane system. Fluid Phase Equilibria 250, 37–48.
Silva-Oliver, G., Eliosa-Jiménez, G., García-Sánchez, F., Avendaño-Gómez, J.R., 2007. High-pressure vapor–liquid equilibria in the nitrogen–n-nonane system. Journal of Supercritical Fluids 42, 36–47.
Stell, G., Rasaiah, J., Narang, H., 1974. Thermodynamic perturbation theory for simple polar fluids. II. Molecular Physics 27, 1393–1414.
Vega, L.F., Vilaseca, O., Llovell, F., Andreu, J.S., 2010. Modeling ionic liquids and the solubility of gases in them: recent advances and perspectives. Fluid Phase Equilibria 294, 15–30.
Ventura, S.P.M., Pauly, J., Daridon, J.L., Marrucho, I.M., Dias, A.M.A., Coutinho, J.A.P., 2007. High-pressure solubility data of methane in aniline and aqueous aniline systems. Journal of Chemical & Engineering Data 52, 1100–1102.
Ventura, S.P.M., Pauly, J., Daridon, J.L., Lopes da Silva, J.A., Marrucho, I.M., Dias, A.M.A., Coutinho, J.A.P., 2008. High pressure solubility data of carbon dioxide in (tri-iso-butyl(methyl)phosphonium tosylate + water) systems. Journal of Chemical Thermodynamics 40, 1187–1192.
Vitu, S., Jaubert, J.-N., Pauly, J., Daridon, J.-L., Barth, D., 2008. Phase equilibria measurements of CO2 + methyl cyclopentane and CO2 + isopropyl cyclohexane binary mixtures at elevated pressures. Journal of Supercritical Fluids 44, 155–163.
Weiss, V.C., Heggen, B., Müller-Plathe, F., 2010. Critical parameters and surface tension of the room temperature ionic liquid [bmim][PF6]: a corresponding-states analysis of experimental and new simulation data. Journal of Physical Chemistry C 114, 3599–3608.
Wertheim, M.S., 1984a. Fluids with highly directional attractive forces. 1. Statistical thermodynamics. Journal of Statistical Physics 35, 19–34.
Wertheim, M.S., 1984b. Fluid with highly directional attractive forces, II. Thermodynamic perturbation theory and integral equations. Journal of Statistical Physics 35, 35–47.
Wertheim, M.S., 1986a. Fluids with highly directional attractive forces.3. Multiple attraction sites. Journal of Statistical Physics 42, 459–476.
Wertheim, M.S., 1986b. Fluids with highly directional attractive forces.4. Equilibrium polymerization. Journal of Statistical Physics 42, 477–492.
Xu, X., Zhao, X., Sun, L., Liu, X., 2009. Adsorption separation of carbon dioxide, methane and nitrogen on monoethanol amine modified β-zeolite. Journal of Natural Gas Chemistry 18, 167–172.
Yokozeki, A., Shiflett, M.B., Junk, C.P., Grieco, L.M., Foo, T., 2008. Physical and chemical absorptions of carbon dioxide in room-temperature ionic liquids. Journal of Physical Chemistry 112, 16654–16663.